Aerosol and Air Quality Research, 14: 260–268, 2014

ISSN: 1680-8584 print / 2071-1409 online
doi: 10.4209/aaqr.2012.12.0360

Impact of Relative Humidity and Water Soluble Constituents of $PM_{2.5}$ on Visibility Impairment in Beijing, China

Jing Chen[1*], Shasha Qiu[2], Jing Shang[1], Ossima M.F. Wilfrid[1], Xingang Liu[1], Hezhong Tian[1], Johan Boman[2]

[1] *State Key Joint Laboratory of Environment Simulation and Pollution Control, School of Environment, Beijing Normal University, Beijing 100875, China*
[2] *Department of Chemistry and Molecular Biology, Division of Atmospheric Science, University of Gothenburg, SE 41296 Göteborg, Sweden*

ABSTRACT

Beijing has been experiencing severe particulate pollution accompanying the fast growing population and economy. This study investigated the impact of $PM_{2.5}$ and its water soluble organic and inorganic constituents on visual impairment in Beijing under different meteorological conditions. According to the analysis of $PM_{2.5}$ samples collected in Spring 2012, water soluble species took up 38.1% of $PM_{2.5}$ mass, among which NO_3^- was the most abundant constituent, followed by SO_4^{2-}, NH_4^+ and water soluble organic matter. The correlation analysis between visibility and aerosol loadings as well as meteorological parameters revealed the dominant impact of meteorological conditions, relative humidity in particular, on visibility impairment over the mass concentration of $PM_{2.5}$. Compared to the total aerosol loading of $PM_{2.5}$, visibility was better correlated with the total mass of water soluble constituents (WSC). The visual range in Beijing was the most sensitive to both WSC and $PM_{2.5}$ in the RH range of 30–70%. Severe visual impairment was observed for RH ≥ 70% with the least sensitivity to WSC and $PM_{2.5}$. The effects of synoptic scale circulation on meteorological variables that affect air quality were also examined with the movement of a cold front as a case study. The findings have direct implications to region-wide policy-making and control strategies.

Keywords: Visibility impairment; Water soluble ion; Water soluble organic carbon; Hygroscopic growth; Synoptic circulation.

INTRODUCTION

Aerosols in the atmosphere can severely impair visibility through the absorption and scattering of light. The light extinction by aerosols depends on their composition and structure (Baumer *et al.*, 2008). The light scattering efficiency of aerosols is a strong function of particle size and aerosols with diameters of 0.5–2 μm are most efficient for scattering visible light. Hygroscopic species such as sulfate and nitrate can increase the water uptake of aerosols, which can shift to a larger size under high-humidity conditions and deteriorate visibility through enhanced light scattering (Chan *et al.*, 1999). Secondary formation of hydrophilic aerosols and their hygroscopic growth have been suggested to be the major causes for the formation of haze in polluted areas (Carrico *et al.*, 2005).

Water soluble inorganic ions along with carbonaceous species especially organic carbon account for a major fraction of $PM_{2.5}$ (Seinfeld and Pandis, 2006; Pathak *et al.*, 2009). Elevated levels of these species have been revealed in hazy weather worldwide. In a visibility study in Los Angeles, Farber *et al.* (1994) found that sulfate followed by nitrate and carbon species were the dominant particulate species in hazy weather. Similar results were reported in Seoul through the chemical analysis of $PM_{2.5}$ in haze episodes (Kang *et al.*, 2004; Geng *et al.*, 2011). In Shanghai, secondary inorganic pollution, dust, and biomass burning were identified as three typical haze types (Du *et al.*, 2011; Huang *et al.*, 2012).

Compared to water soluble inorganic ions, the lower hygroscopicity of the organic species can lead to less sensitivity of visibility degradation to ambient relative humidity (Carrico *et al.*, 2005; Levin *et al.*, 2009). The hygroscopic growth of fine aerosols attributable to particulate organic matter (POM), when considered as a whole, was often negelected in model calculations of aerosol light extinction coefficients (Cheung *et al.*, 2005; Odman *et al.*, 2009). However, water soluble organic matter (WSOM) can take up a significant portion of POM, especially in polluted areas where secondary aerosol formation is facilitated (Yang *et al.*, 2005; Huang *et al.*, 2006). Unlike the non-water

* Corresponding author.
Tel.: 86-10-58804585; Fax: 86-10-58804585
E-mail address: jingchen@bnu.edu.cn

soluble portion of POM, WSOM is more hydrophilic and its effects on the hygroscopic growth of fine aerosols as well as visual impairment need to be studied explicitly.

Because of high industrial emissions, increased dependence on private motor vehicles associated with growing population, and natural topographical and meteorological conditions, Beijing has been experiencing severe particulate pollution and frequent haze episodes. A number of studies on atmospheric particulate matter in Beijing have reported high levels of $PM_{2.5}$ and particulate salts and organics (He *et al.*, 2001; Wang *et al.*, 2005; Chan and Yao, 2008; Zhou *et al.*, 2012). Previous studies also found that visibility in Beijing was negatively correlated to the $PM_{2.5}$ mass concentration (Sun *et al.*, 2006; Zhou *et al.*, 2012). Zhang *et al.* (2010) investigated the temporal variation of visibility in Beijing from 1999 to 2007 as well as its dependence on relative humidity and PM_{10} and found that the increase of RH would result in visibility degradation despite of decreasing levels of PM_{10}.

The goal of this paper is to investigate the mechanism of visual impairment in Beijing from the chemical view of $PM_{2.5}$ and its water soluble organic and inorganic constituents under different meteorological conditions, so as to elucidate the combined effects of relative humidity and $PM_{2.5}$ on visibility degradation.

EXPERIMENTAL

Study Area

Beijing, the capital of China, is located at 39°56'N and 116°20'E in a warm temperate zone with typical continental monsoon climate. The population in Beijing has increased from 13.6 million in 2000 to 19.6 million in 2010; meanwhile, the gross domestic product (GDP) has increased from 38.2 billion dollars in 2000 to 208.5 billion dollars in 2010 (Beijing Statistical Yearbook, 2011). Accompanying the growth of population and development of economy, the annual energy consumption in Beijing has also increased, with obvious transition of the energy structure from coal dominant to clean energy dominant as shown in Fig. 1. The number of civil motor vehicles in Beijing showed an accelerating growth from 2005 to 2010 and reached 4.8 million by the end of 2010. In 2011 the Beijing government started to limit new car registrations to 20,000 annually so as to ease the traffic and pollution pressure. Fig. 1 also shows the temporal variation of the occurrence frequency of daily averaged visibility in different ranges in Beijing. Hazy weather is common in Beijing with daily averaged visibility less than 10 km on over 50% of the days annually.

Sampling

Atmospheric measurements were carried out on the campus of Beijing Normal University located between the 2nd and 3rd Ring Roads in the north of Beijing downtown area, which represents a typical urban environment in Beijing. The sampling station was situated on the roof of a six-floor building, about 20 m above ground. $PM_{2.5}$ samples were collected on quartz filters (Whatman, 20.3 × 25.4 cm) by a high-volume air sampler at a flow rate of 1.05 m^3/min (Wuhan Tianhong Instruments Co., Ltd., TH-1000C). Aerosol sampling was carried out in Spring 2012 (March and April) with the collection of separate day-time and night-time samples. The day-time samples were collected from 7:00 to 19:00 and the night-time samples from 19:00 to 7:00 the next day. No aerosol sampling was performed on rainy days. A total of 30 $PM_{2.5}$ samples were collected and analyzed in this study, including 15 day-time samples and 15 night-time samples. The filters were carefully folded and weighed before and after sampling with an analytical balance (Sartorius, BT 125D) after stabilizing under constant temperature (20°C) and relative humidity (40%) to determine the mass of $PM_{2.5}$ (Wang *et al.*, 2005). After the mass measurement, the samples were stored in polyethylene bags and preserved in a refrigerator for further analysis.

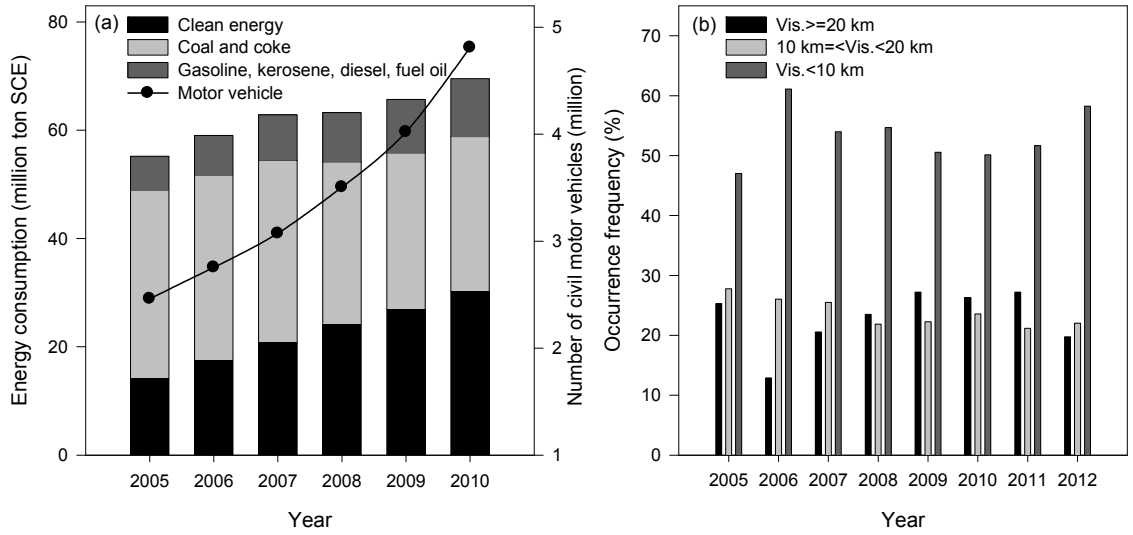

Fig. 1. (a) Annual energy consumption in million tons of standard coal equivalent (SCE) and total number of civil motor vehicles in Beijing (data source: Beijing Statistical Yearbook). (b) Annual occurrence frequency of daily averaged visibility in different ranges in Beijing (data source: www.wunderground.com).

Meteorological parameters including pressure, temperature, relative humidity, wind speed, gust speed, wind direction, solar radiation and precipitation were simultaneously recorded by an automatic meteorological station (MetOne Instruments, Inc.) at the sampling site with 30-min time resolution. Atmospheric visibility was measured with a visibility sensor (Belfort Model 6000, visual range: 200 m–50 km) with 1-min time resolution. The day-time and night-time average values of the meteorological parameters and visibility were obtained as the arithmetic mean of the raw data.

Chemical Analysis

One-fourth of each sample filter as well as a blank filter was extracted with 30 mL deionized water ultrasonically for 40 min. The extract was centrifuged and passed through a microporous membrane with a pore size of 0.45 μm and further analyzed for the ionic composition (Wang *et al.*, 2005) and dissolved organic carbon (Wang *et al.*, 2002) respectively. The ionic analysis was performed by ion chromatography (Dionex 600) to determine the concentration of inorganic ions as well as oxalic acid. Five cations including NH_4^+, Ca^{2+}, K^+, Mg^{2+}, Na^+ and five anions including NO_3^-, SO_4^{2-}, Cl^-, NO_2^-, $C_2O_4^{2-}$ were measured. The recovery of each ion ranged between 83% and 107%. The amount of dissolved organic carbon in the extract was measured by a laboratory TOC analyzer (GE, Sievers 900). The blank values were subtracted from sample measurements.

Aerosol Water Content Calculation

Aerosol water uptake can have a large effect on light scattering by altering particle size and refractive index. As an indicator of the mutual effects of RH and water soluble constituents in $PM_{2.5}$, aerosol water content was calculated using the online Aerosol Inorganics Model (AIM) (website: www.aim.env.uea.ac.uk/aim/aim.php) (Wexler and Clegg, 2002). AIM-II was employed with temperature, RH, H^+, NH_4^+, SO_4^{2-}, NO_3^- as the major input. Oxalic acid was selected to represent organic compounds. The H^+ input in the model was calculated as: $[H^+]_{measure} = 2[SO_4^{2-}]_{measure} + [NO_3^-]_{measure} - [NH_4^+]_{measure}$ (Cheng *et al.*, 2011).

RESULTS AND DISCUSSION

Composition of Water Soluble Species in $PM_{2.5}$

$PM_{2.5}$ samples were collected and analyzed for the water soluble organic and inorganic constituents in Spring 2012. Water soluble organic matter in $PM_{2.5}$ tends to be more oxygenated than the non-water soluble portion of POM; thus the mass concentration of WSOM was estimated by multiplying the measured mass concentration of organic carbon by a factor of 2.1, as suggested by Turpin and Lim (Turpin and Lim, 2001). Accordingly, the total mass concentration of the water soluble constituents (WSC) of $PM_{2.5}$ can be calculated as the sum of the mass concentrations of WSOM and inorganic ions. Fig. 2 shows the temporal variation of the mass concentrations of $PM_{2.5}$ and WSC during the sampling period of Spring 2012. The spring of Beijing is characterized by frequent strong northwestern wind, which could either clean up the local air pollutants or carry dust from the Gobi desert to Beijing and lead to high dust concentrations (Chan and Yao, 2008). Crustal species such as Si, Al, Ca, Fe generally dominate in the aerosols that are regionally transported from the north and the west (Sun *et al.*, 2005). As a result, the $PM_{2.5}$ concentration during the sampling period varied significantly, ranging between 55.9–668.7 μg/m; WSC took around 38% of $PM_{2.5}$ mass and showed a smaller variation range between 11.28–169.06 $\mu g/m^3$. The day-time average concentrations of $PM_{2.5}$ and WSC (250.9 $\mu g/m^3$ and 80.41 $\mu g/m^3$ respectively) were both higher than the night-time concentrations (168.9 $\mu g/m^3$ and 68.30 $\mu g/m^3$ respectively), indicating higher source contributions in the day time.

Accompanying the varying aerosol concentration and composition as well as meteorological conditions, the visual range in the sampling period varied significantly from 1.3 km to 47.0 km, as shown in Fig. 2. Table 1 shows the average concentration of the analyzed water soluble species in $PM_{2.5}$ on clear (visibility ≥ 20 km), moderate (20 km > visibility ≥ 10 km), and hazy (visibility < 10 km) days respectively. The concentration of each water soluble species in $PM_{2.5}$ was greatly enhanced on hazy days, with an exception of Ca^{2+} which was closely related to regional transport of mineral dust to Beijing.

Table 1 also shows the average mass percentages of each water soluble species in the total mass of WSC and $PM_{2.5}$. NO_3^- was the most abundant water soluble species in $PM_{2.5}$, followed by SO_4^{2-}, NH_4^+ and WSOM. The formation of NO_3^- and SO_4^{2-} mainly come from the oxidation of precursor gases, i.e., NO_x and sulfur dioxide. Coal combustion is the major source of sulfur dioxide while NO_x can be produced in various combustion processes such as coal combustion and vehicular emissions. It has been reported that gaseous ammonia could be neutralized by atmospheric nitric acid and acidic sulfate particles to form NH_4^+ (Yang *et al.*, 2005; Ianniello *et al.*, 2011). NH_4^+ showed high correlation coefficients with NO_3^- (0.91) and SO_4^{2-} (0.93) in this study, which was consistent with the proposed formation mechanism of particulate NH_4^+.

The historical concentrations of major inorganic ions in $PM_{2.5}$ in the spring of Beijing have been reported in previous studies (He *et al.*, 2001; Wang *et al.*, 2005; Zhou *et al.*, 2012). As shown in Table 2, $PM_{2.5}$ and its major ions exhibited an increasing trend in general. Besides, the molar ratio of NO_3^- to SO_4^{2-} increased from 1.11 in 2000 to 2.01 in 2012, consistent with the rapid increase of the number of motor vehicles in Beijing (Fig. 1). The equivalent concentration ratio of NH_4^+ to the sum of NO_3^- and SO_4^{2-} was smaller than 1 throughout the years, indicating the acidic nature of $PM_{2.5}$ in Beijing. According to a recent study on $PM_{2.5}$ acidity, the acidity of $PM_{2.5}$ in megacities was closely related to the formation of NO_3^-, which was enhanced due to the growing emission of NO_x by motor vehicles (He *et al.*, 2012).

The mass concentration of water soluble organic matter was comparable to that of the major inorganic ions in $PM_{2.5}$, taking 16.2% of WSC and 5.0% of $PM_{2.5}$. Oxalate, the dominant ion of dicarboxylic acids, accounted for around 3% of WSOM. Oxalate is generally believed to be

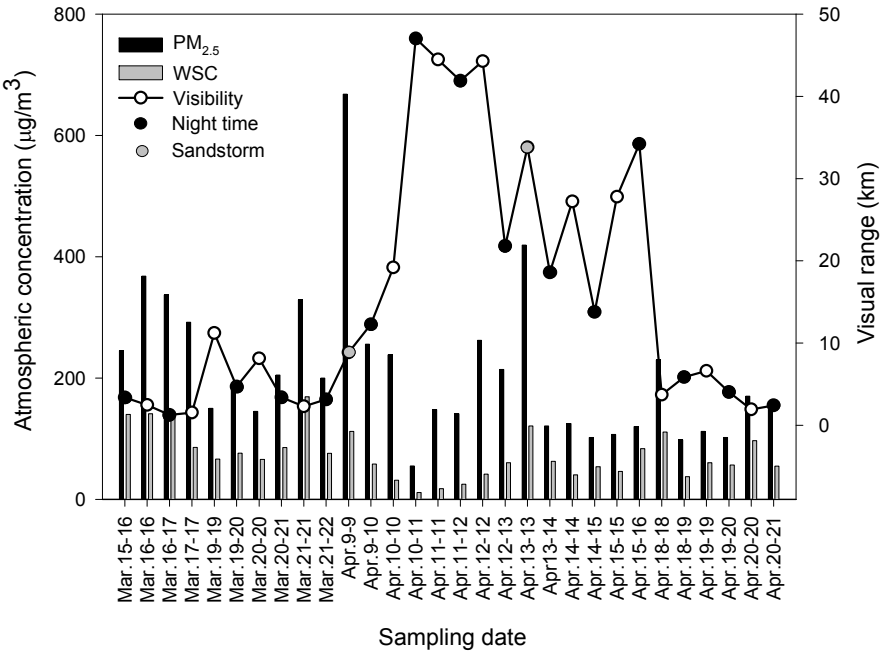

Fig. 2. Variation of the total mass concentrations of $PM_{2.5}$ and its water soluble constituents (WSC) as well as the visual range in Beijing during the sampling period of Spring 2012.

Table 1. Mean and standard deviation of the concentrations ($\mu g/m^3$) of water soluble species and their mass percentages in the total mass of water soluble constituents and $PM_{2.5}$ in Beijing in Spring 2012.

Species	Vis. ≥ 20 km (N = 8)	20 km > Vis. ≥ 10 km (N = 6)	Vis. < 10 km (N = 16)	All samples (N = 30)		
	Mean ± SD ($\mu g/m^3$)	Mean ± SD ($\mu g/m^3$)	Mean ± SD ($\mu g/m^3$)	Mean ± SD ($\mu g/m^3$)	%WSC ± SD (%)	%$PM_{2.5}$ ± SD (%)
NO_3^-	16.64 ± 14.62	16.80 ± 5.75	31.96 ± 13.27	24.84 ± 14.43	32.2 ± 6.4	12.8 ± 6.2
SO_4^{2-}	9.65 ± 10.60	15.12 ± 4.07	25.32 ± 11.01	19.10 ± 11.92	23.9 ± 7.1	9.6 ± 4.7
Cl^-	2.70 ± 1.68	2.24 ± 0.87	5.24 ± 3.08	3.96 ± 2.77	5.3 ± 1.7	1.9 ± 0.9
$C_2O_4^-$	0.23 ± 0.14	0.33 ± 0.08	0.33 ± 0.11	0.31 ± 0.12	0.5 ± 0.2	0.2 ± 0.1
NO_2^-	0.14 ± 0.10	0.18 ± 0.07	0.16 ± 0.09	0.16 ± 0.08	0.3 ± 0.2	0.1 ± 0.0
NH_4^+	7.44 ± 6.08	7.99 ± 3.23	17.00 ± 7.73	12.65 ± 8.00	16.2 ± 4.7	6.7 ± 3.7
Ca^{2+}	2.78 ± 2.36	2.46 ± 0.79	2.08 ± 1.86	2.34 ± 1.83	3.9 ± 2.9	1.2 ± 0.5
K^+	0.72 ± 0.92	0.73 ± 0.33	1.59 ± 0.74	1.19 ± 0.84	1.4 ± 0.7	0.6 ± 0.5
Mg^{2+}	0.30 ± 0.43	0.31 ± 0.17	0.44 ± 0.29	0.38 ± 0.32	0.5 ± 0.3	0.2 ± 0.1
Na^+	0.15 ± 0.29	0.003 ± 0.004	0.23 ± 0.35	0.16 ± 0.30	0.1 ± 0.3	0.1 ± 0.1
WSOM	7.73 ± 4.33	9.65 ± 4.44	10.47 ± 4.29	9.58 ± 4.34	16.2 ± 11.6	5.0 ± 2.1
WSC	48.25 ± 36.88	55.47 ± 12.50	94.50 ± 38.34	74.36 ± 40.01	-	38.1 ± 15.1
$PM_{2.5}$	172.1 ± 115.6	180.2 ± 64.4	239.9 ± 142.2	209.9 ± 124.4	-	-

Table 2. Mean (and standard deviation) of the historical spring time concentrations of major inorganic ions in $PM_{2.5}$ in Beijing.

Year	$PM_{2.5}$ ($\mu g/m^3$)	SO_4^{2-} ($\mu g/m^3$)	NO_3^- ($\mu g/m^3$)	NH_4^+ ($\mu g/m^3$)	$\frac{[NO_3^-]}{[SO_4^{2-}]}$	$\frac{[NH_4^+]}{[NO_3^-]+2[SO_4^{2-}]}$	Reference
2000	88.6	10.15	7.26	4.28	1.11	0.72	He *et al.*, 2001
2001–2003	162.06 ± 179.94	13.52 ± 13.95	11.92 ± 11.79	6.47 ± 6.75	1.37	0.76	Wang *et al.*, 2005
2006	269.9 ± 109.9	15.2 ± 9.4	13.8 ± 10.4	2.9 ± 3.7	1.41	0.30	Zhou *et al.*, 2012
2012	209.9 ± 124.4	19.10 ± 11.92	24.84 ± 14.43	12.65 ± 8.00	2.01	0.88	This study

formed by in-cloud processes (Kawamura *et al.*, 2010). In addition, the formation of secondary organic aerosols including oxalate could be enhanced under high-humidity conditions similar to the in-cloud process (Hennigan *et al.*, 2008). Good correlation was found between oxalate and NO_3^- or SO_4^{2-} with correlation coefficients (r) of 0.84 and

0.76 respectively, indicating similar secondary formation processes of these species such as the in-cloud process. WSOM comes from a variety of different sources, such as primary emissions from biomass burning, fossil fuel combustion, and photochemical oxidation of organic precursors originated from both anthropogenic and biogenic sources (Chebbi and Carlier, 1996). Due to the inherent complexity of WSOM associated with various sources and structures, WSOM was less correlated with NO_3^- (r: 0.55) and SO_4^{2-} (r: 0.56). The correlation coefficient between WSOM and oxalate was 0.62.

Impact of Meteorological Conditions on Visibility Impairment

Table 3 lists the correlation coefficients of visibility with major water soluble species in $PM_{2.5}$ and meteorological parameters. The highest correlation was observed between visibility and relative humidity, with a correlation coefficient of –0.83. Visibility was positively correlated to temperature and wind speed, indicating visibility improvement under favorable weather conditions for pollutant dispersion. Based on a long-term observation in Beijing covering four seasons in 2006, Zhou *et al.* (2012) reported similar results on the correlation of visibility with relative humidity (–0.53) and wind speed (0.54) but a weak negative correlation with temperature (–0.20). Higher atmospheric temperature can not only facilitate the atmospheric dispersion of pollutants but also promote the formation of secondary aerosols, which exert opposite effects on atmospheric visibility. As shown in our study, the former effect dominates in spring with moderate temperature, resulting in a positive correlation between visibility and temperature. However, the latter effect takes a leading role in summer with high temperature, resulting in a negative correlation. As a net outcome of both effects, the atmospheric visibility showed a weak negative correlation with temperature in the long-term observation (Zhou *et al.*, 2012).

Among the analyzed water soluble species, visibility degradation in Beijing showed the highest dependence on SO_4^{2-}, followed by NH_4^+ and NO_3^-. Compared to the major inorganic ions, the concentration of water soluble organic matter varied in a smaller range and was less correlated with visibility. In spite of the varying correlation coefficients between visibility and different water soluble species, the total mass of water soluble constituents showed good correlation with visibility, as opposed to both $PM_{2.5}$ and the rest water insoluble portion of $PM_{2.5}$. Aerosols with size around 550 nm are most efficient visible light scatterers, therefore, the good correlation of visibility with WSC probably resulted from the accumulation of WSC, the majority of which were secondary species, in the sub-micron size that contributes greatly to visibility degradation. Cheng *et al.* (2011) studied the size distributions of water soluble ions in aerosols in Jinan, China and evidenced the accumulation of SO_4^{2-}, NH_4^+ and NO_3^- in fine mode of 0.18–1.0 μm. As shown in Table 3, the correlation of visibility with WSC plus particulate water was further improved compared to that with WSC. More details on the effects of particulate water are presented in the next section. It is noteworthy that the poor correlation between the $PM_{2.5}$ residual and visibility does not necessarily suggest negligible impact of other chemical components in $PM_{2.5}$ on visibility degradation in Beijing. For example, the contribution of organic carbon (both water soluble and insoluble) and elemental carbon in $PM_{2.5}$ to total light extinction was 12.3% and 6.9% respectively during the polluted period in Beijing, as reported by Jung *et al.* (2009). However, the different physicochemical properties and concentration trends of various chemical components in the $PM_{2.5}$ residual, such as crustal species, water insoluble organic carbon and elemental carbon, probably masked the effect of a single specific component of the $PM_{2.5}$ residual on visibility degradation and resulted in the poor correlation between the $PM_{2.5}$ residual and visibility.

Visibility in Beijing exhibited an obvious diel pattern with the day-time average (16.2 km) higher than the night-time (14.5 km), as shown in Fig. 2. The meteorological conditions in Beijing were usually more stagnant at night, as characterized by lower temperature, lower wind speed and higher relative humidity. On the other hand, the night-time concentrations of $PM_{2.5}$ and its water soluble constituents were generally lower due to the lessened source contributions (Fig. 2). Consistent with the results of the correlation analysis, the lower visibility at night associated with more stagnant meteorological conditions and lower $PM_{2.5}$ concentrations suggested the dominant impact of meteorological conditions on visibility impairment over the mass concentrations of $PM_{2.5}$ in the study period in Beijing.

It is known that high relative humidity could not exert a large effect on visibility impairment if the aerosol mass loading reduces to a low level, except in the foggy days when relative humidity is usually larger than 90%. However, in the context of high aerosol mass loading (average $PM_{2.5}$ concentration of 209.9 $\mu g/m^3$) in the study period in Beijing, relative humidity turned out to be the most influencing factor on visual impairment as indicated by the correlation analysis. The formation of secondary aerosol species such as NO_3^-, SO_4^{2-} and secondary organic compounds could be enhanced under high-humidity conditions similar to the in-cloud process (Yu *et al.*, 2005; Hennigan *et al.*, 2008). Besides, such fine hydrophilic aerosols could shift to a larger size by taking ambient water vapor, resulting in higher extent of light scattering and visibility degradation (Chan *et al.*, 1999; Xiao *et al.*, 2011; Liu *et al.*, 2012). The hygroscopic growth of fine aerosols is determined by both ambient relative humidity and particle hydrophilicity, signifying the importance of water soluble species in $PM_{2.5}$ at given relative humidity.

Table 3. Correlation coefficients of visibility with major water soluble species in $PM_{2.5}$ and meteorological parameters.

	NO_3^-	SO_4^{2-}	NH_4^+	WSOM	WSC	H_2O	WSC plus H_2O	Rest of $PM_{2.5}$	$PM_{2.5}$	Temp.	RH	Wind speed
r	–0.54	–0.65	–0.62	–0.23	–0.57	–0.49	–0.62	–0.04	–0.22	0.53	–0.83	0.48

Impact of Water Soluble Species on Visibility Impairment under Different RH

Fig. 3 shows the variation of visibility with relative humidity and the atmospheric concentrations of particulate water, WSC, WSC plus particulate water, and $PM_{2.5}$. Particulate water content was calculated by the online AIM model based on ambient temperature, relative humidity and concentrations of major inorganic ions. Oxalic acid was selected to represent organic compounds. Inclusion of oxalic acid in the calculation resulted in less than 1% increase of the calculated aerosol water content due to the low proportion of oxalic acid in the water soluble constituents of $PM_{2.5}$. The complexity of WSOM composition inhibited the accurate calculation of the water content associated with WSOM by the AIM model. However, the sum of water soluble organic matter in $PM_{2.5}$ was considerable and should be taken into account for aerosol water uptake and subsequent hygroscopic growth. Considering the good correlation between visibility and WSC as shown in Table 3, the impact of water soluble species on visibility impairment was investigated taking the water soluble constituents of $PM_{2.5}$ as a whole.

Power function fitting was conducted between visibility and the influencing factors, as shown in Fig. 3. The best fitting was observed between visibility and relative humidity. As relative humidity increases, the visual range quickly decreases. However, the aerosol water content did not increase much until beyond 70% RH. The dependence of visibility on aerosol water content suggests that water vapor uptake by fine aerosols matters in the hygroscopic growth regime below 70% RH even if the total mass of water is low. As the ambient relative humidity goes beyond 70%, activation of the aerosol particle would occur, resulting in greatly enhanced aerosol water content and severe visibility impairment. WSC was better fitted with visibility than $PM_{2.5}$, confirming the importance of water soluble species in visual impairment. What's more, the fitting was further improved between visual range and WSC plus particulate water, which reflected the significant impact of the hygroscopic growth of fine hydrophilic aerosols on visual impairment.

According to the AIM calculation result, the aerosol water content was extremely low below 30% RH, indicating negligible hygroscopic growth of aerosols; on the other hand, activation of the aerosol particle would occur beyond 70% RH. Therefore, the dependence of visibility on $PM_{2.5}$ and its water soluble constituents was investigated in three different regimes of RH. Fig. 4 shows the power function fitting between the visual range and the atmospheric concentrations of WSC and $PM_{2.5}$ in different RH ranges in Beijing. The visual range in Beijing was the most sensitive to both WSC and $PM_{2.5}$ in the RH range of 30–70%, where equilibrium water uptake occurred. Severe visual impairment was observed for RH $\geq$ 70%, where the visual range showed the least sensitivity to WSC and $PM_{2.5}$.

According to the fitting curves shown in Fig. 4, the mass concentration of WSC or $PM_{2.5}$ in Beijing should be below 57 $\mu g/m^3$ or 147 $\mu g/m^3$ in order to avoid the occurrence of haze (visibility < 10 km) for RH > 70%. The limits are restricted to 16 $\mu g/m^3$ (WSC) and 39 $\mu g/m^3$ ($PM_{2.5}$) respectively for RH $\geq$ 70%. Further improvement of visibility requires more efforts in the control and reduction of $PM_{2.5}$ and its water soluble constituents in Beijing.

Impact of Synoptic Circulation on Visibility Impairment

The meteorological variables that affect air quality are strongly modulated by the synoptic scale circulation (Huth *et al.*, 2008; Zhang *et al.*, 2012). Beijing is surrounded by the Taihang Mountain in the west and the Yanshan Mountain in the north and northeast, whereas the south is connected to the Great North China Plain. Due to the unique

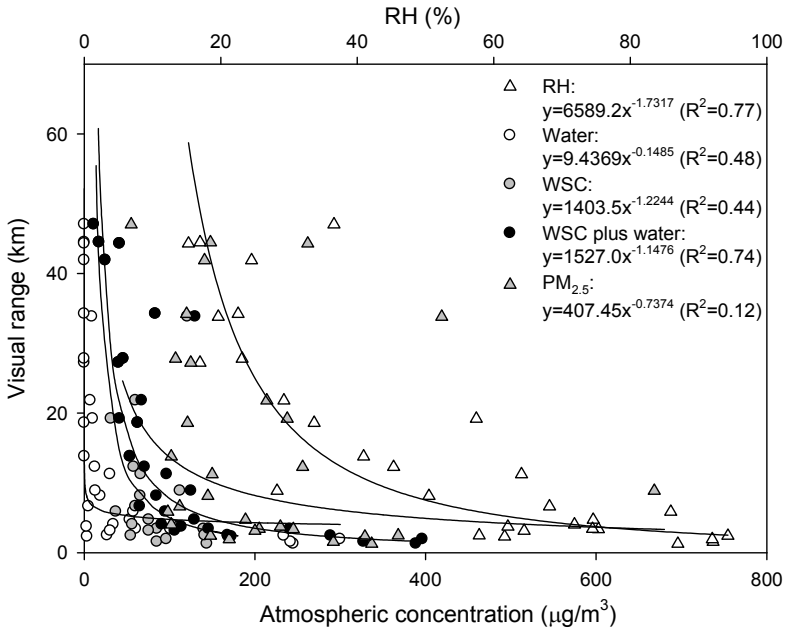

Fig. 3. The power function fitting between the visual range and RH, the atmospheric concentrations of particulate water, the total water soluble constituents, the total water soluble constituents plus particulate water, and $PM_{2.5}$ in Beijing.

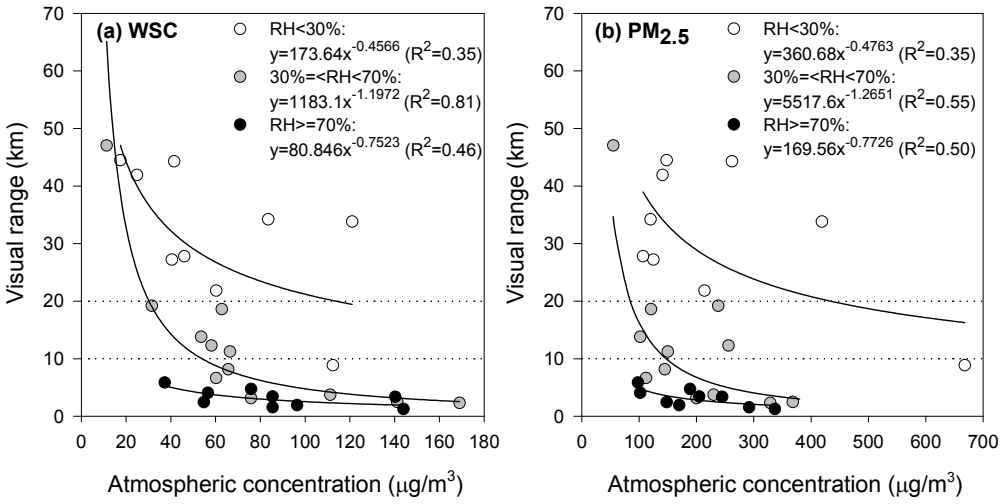

Fig. 4. The power function fitting between the visual range and the atmospheric concentrations of the total water soluble constituents and $PM_{2.5}$ in different RH ranges in Beijing.

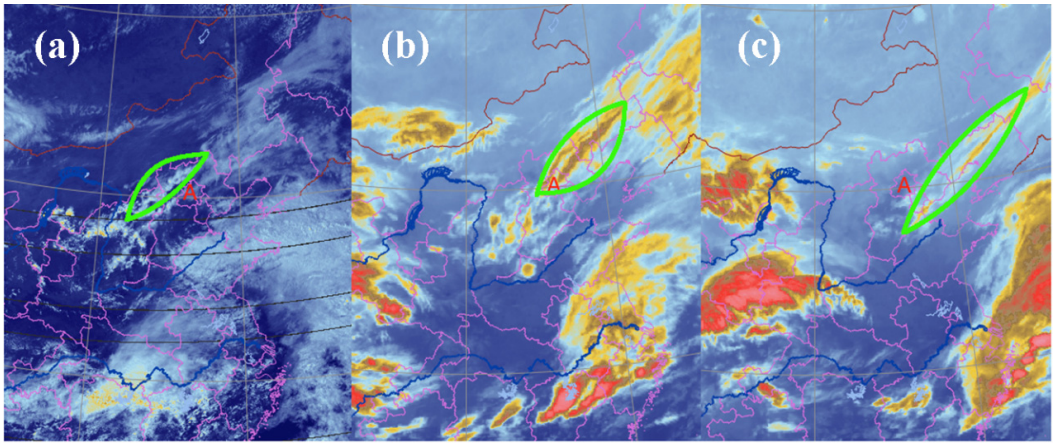

Fig. 5. The satellite cloud images at (a) April 10th, 14:00, (b) April 10th, 20:00, and (c) April 11th, 02:00 (provided by China Meteorological Administration). Beijing is marked with "A".

topography of Beijing, the air quality is highly dependent on the weather conditions driven by the day-to-day synoptic circulation variability. In this study, great improvement of visibility was observed during April 10th–12th (Fig. 2), which was closely related to a cold front weather system. Fig. 5 illustrates the movement of the cold front by satellite cloud images. Moderate visibility and high concentrations of $PM_{2.5}$ were observed in the day time of April 10th under the pre-frontal conditions. The cold front arrived in Beijing at around 6:00 p.m., resulting in a short shower. The $PM_{2.5}$ concentration was significantly reduced afterwards and the visibility in Beijing was greatly improved in the clean and dry atmosphere.

Dry and cold winter monsoons from Siberia and Mongolia prevail in Beijing from September to next April. Except for extreme dust storm events, the prevailing northwestern wind and dry weather during this period are generally favorable for the improvement of visibility in Beijing. However, accumulation of water soluble species of $PM_{2.5}$ in the atmosphere would quickly deteriorate the situation as soon as the ambient relative humidity increases.

CONCLUSIONS

According to the analysis of $PM_{2.5}$ samples collected in Spring 2012, it was found that Beijing was heavily polluted by $PM_{2.5}$ with an average of 209.9 μg/m^3. Water soluble species took up 38.1% of $PM_{2.5}$ mass, among which NO_3^- was the most abundant constituent, followed by SO_4^{2-}, NH_4^+ and water soluble organic matter. The high ratio of NO_3^- to SO_4^{2-} reflected the growing emissions by motor vehicles in Beijing. The concentrations of major water soluble species in $PM_{2.5}$ were all greatly enhanced in hazy days.

Both aerosol loadings and meteorological conditions could affect the visual range in Beijing. According to the correlation analysis, the impact of meteorological conditions on visibility impairment dominated over the mass concentration of $PM_{2.5}$ in the context of high aerosol mass loading in the study period in Beijing. The highest correlation was observed between visibility and relative humidity, with a correlation coefficient of –0.83. Compared to the total aerosol loading of $PM_{2.5}$, visibility was better correlated with the total mass of water soluble species. The

visual range in Beijing was the most sensitive to both WSC and $PM_{2.5}$ in the RH range of 30–70%. Severe visual impairment was observed for RH ≥ 70%, where the visual range showed the least sensitivity to WSC and $PM_{2.5}$. In order to avoid the occurrence of haze (visibility < 10 km) in Beijing under relatively humid conditions, the limits for the mass concentrations of WSC and $PM_{2.5}$ should be restricted to 16 μg/m^3 and 39 μg/m^3 respectively.

The synoptic circulation strongly modulates the weather conditions in Beijing and affects the air quality. The prevailing northwestern wind and dry weather in the spring are favorable for the improvement of visibility in Beijing. However, the visibility is fragile due to the high atmospheric concentrations of water soluble species of $PM_{2.5}$ caused by the accumulation of anthropogenic emissions. Strict pollution control and emission reduction will be needed to improve the air quality and visibility in Beijing.

ACKNOWLEDGMENTS

This work was supported by National Natural Science Foundation of China (No. 40905054).

REFERENCES

Baumer, D., Vogel, B., Versick, S., Rinke, R., Mohler, O. and Schnaiter, M. (2008). Relationship of Visibility, Aerosol Optical Thickness and Aerosol Size Distribution in an Ageing Air Mass over South-West Germany. *Atmos. Environ.* 42: 989–998.

Carrico, C.M., Kreidenweis, S.M., Malm, W.C., Day, D.E., Lee, T., Carrillo, J., McMeeking, G. R. and Collett, J.L.J. (2005). Hygroscopic Growth Behavior of a Carbon-Dominated Aerosol in Yosemite National Park. *Atmos. Environ.* 39: 1393–1404.

Chan, C.K. and Yao, X. (2008). Air Pollution in Mega Cities in China. *Atmos. Environ.* 42: 1–42.

Chan, Y.C., Simpson, R.W., Mctainsh, G.H., Vowles, P.D., Cohen, D.D. and Bailey, G.M. (1999). Source Apportionment of Visibility Degradation Problems in Brisbane (Australia) Using the Multiple Linear Regression Techniques. *Atmos. Environ.* 33: 3237–3250.

Chebbi, A. and Carlier, P. (1996). Carboxylic Acids in the Troposphere, Occurrence, Sources, and Sinks: a Review. *Atmos. Environ.* 30: 4233–4249.

Cheng, S., Yang, L., Zhou, X., Xue, L., Gao, X., Zhou, Y. and Wang, W. (2011). Size-Fractionated Water-Soluble Ions, Situ pH and Water Content in Aerosol on Hazy Days and the Influences on Visibility Impairment in Jinan, China. *Atmos. Environ.* 45: 4631–4640.

Cheung, H.C., Wang, T., Baumann, K. and Guo, H. (2005). Influence of Regional Pollution Outflow on the Concentrations of Fine Particulate Matter and Visibility in the Coastal Area of Southern China. *Atmos. Environ.* 39: 6463–6474.

Du, H., Kong, L., Cheng, T., Chen, J., Du, J., Li, L., Xia, X., Leng, C. and Huang, G. (2011). Insights into Summertime Haze Pollution Events over Shanghai Based on Online Water-soluble Ionic Composition of Aerosols. *Atmos. Environ.* 45: 5131–5137.

Farber, R.J., Welsing, P.R. and Rozzi, C. (1994). PM_{10} and Ozone Control Strategy to Improve Visibility in the Los Angeles Basin. *Atmos. Environ.* 28: 3277–3283.

Geng, H., Ryu, J.Y., Maskey, S., Jung, H.J. and Ro, C.U. (2011). Characterisation of Individual Aerosol Particles Collected during a Haze Episode in Incheon, Korea Using the Quantitative ED-EPMA Technique. *Atmos. Chem. Phys.* 11: 1327–1337.

He, K., Yang, F., Ma, Y., Zhang, Q., Yao, X., Chan, C. K., Cadle, S., Chan, T. and Mulawa, P. (2001). The Characteristics of $PM_{2.5}$ in Beijing, China. *Atmos. Environ.* 35: 4959–4970.

He, K., Zhao, Q., Ma, Y., Duan, F., Yang, F., Shi, Z. and Chen, G. (2012). Spatial and Seasonal Variability of $PM_{2.5}$ Acidity at Two Chinese Megacities: Insights into the Formation of Secondary Inorganic Aerosols. *Atmos. Chem. Phys.* 12: 1377–1395.

Hennigan, C.J., Bergin, M.H., Dibb, J.E. and Weber, R.J. (2008). Enhanced Secondary Organic Aerosol Formation due to Water Uptake by Fine Particles. *Geophys. Res. Lett.* 35: L18801.

Huang, K., Zhuang, G., Lin, Y., Fu, J. S., Wang, Q., Liu, T., Zhang, R., Jiang, Y., Deng, C., Fu, Q., Hsu, N.C. and Cao, B. (2012). Typical Types and Formation Mechanisms of Haze in an Eastern Asia Megacity, Shanghai. *Atmos. Chem. Phys.* 12: 105–124.

Huang, X.F., He, L.Y., Hu, M. and Zhang, Y.H. (2006). Annual Variation of Particulate Organic Compounds in $PM_{2.5}$ in the Urban Atmosphere of Beijing. *Atmos. Environ.* 40: 2449–2458.

Huth, R., Beck, C., Philipp, A., Demuzere, M., Ustrnul, Z., Cahynová, M., Kyselý, J. and Tveito, O.E. (2008). Classifications of Atmospheric Circulation Patterns. *Ann. N.Y. Acad. Sci.* 1146: 105–152.

Ianniello, A., Spataro, F., Esposito, G., Allegrini, I., Hu, M. and Zhu, T. (2011). Chemical Characteristics of Inorganic Ammonium Salts in $PM_{2.5}$ in the Atmosphere of Beijing (China). *Atmos. Chem. Phys.* 11: 10803–10822.

Jung, J., Lee, H., Kim, Y.J., Liu, X., Zhang, Y., Hu, M. and Sugimoto, N. (2009). Optical Properties of Atmospheric Aerosols Obtained by in Situ and Remote Measurements during 2006 Campaign of Air Quality Research in Beijing (CAREBeijing-2006). *J. Geophys. Res.* 114: D00G02, doi: 10.1029/2008JD010337.

Kang, C.M., Lee, H.S., Kang, B.W., Lee, S.K. and Sunwoo, Y. (2004). Chemical Characteristics of Acidic Gas Pollutants and $PM_{2.5}$ Species during Hazy Episodes in Seoul, South Korea. *Atmos. Environ.* 38: 4749–4760.

Kawamura, K., Kasukabe, H. and Barrie, L.A. (2010). Secondary Formation of Water-Soluble Organic Acids and α-Dicarbonyls and Their Contributions to Total Carbon and Water-Soluble Organic Carbon: Photochemical Aging of Organic Aerosols in the Arctic spring. *J. Geophys. Res.* 115: D21306.

Levin, E.J.T., Kreidenweis, S.M., McMeeking, G.R., Carrico, C.M., Collett, J.L.J. and Malm, W.C. (2009). Aerosol Physical, Chemical and Optical Properties during the Rocky Mountain Airborne Nitrogen and Sulfur study.

Atmos. Environ. 43: 1932–1939.

Liu, X., Zhang, Y., Cheng, Y., Hu, M. and Han, T. (2012). Aerosol Hygroscopicity and Its Impact on Atmospheric Visibility and Radiative Forcing in Guangzhou during the 2006 PRIDE-PRD Campaign. *Atmos. Environ.* 60: 59–67.

Odman, M.T., Hu, Y., Russell, A.G., Hanedar, A., Boylan, J. and Brewer, P.F. (2009). Quantifying the Sources of Ozone, Fine Particulate Matter, and Regional Haze in the Southeastern United States. *J. Environ. Manage.* 90: 3155–3168.

Pathak, R.K., Wu, W.S. and Wang, T. (2009). Summertime $PM_{2.5}$ Ionic Species in four Major Cities of China: Nitrate Formation in an Ammonia-deficient Atmosphere. *Atmos. Chem. Phys.* 9: 1711–1722.

Seinfeld, J.H. and Pandis, S.N. (2006). *Atmospheric Chemistry and Physics: From Air Pollution to Climate Change*, 2nd ed., John Wiley & Sons, New York, USA.

Sun, Y., Zhuang, G., Wang, Y., Zhao, X., Li, J., Wang, Z. and An, Z. (2005). Chemical Composition of Dust Storms in Beijing in Implications for Mixing of Mineral Aerosol with Pollution Aerosol on the Pathway. *J. Geophys. Res.* 110: D24209.

Sun, Y., Zhuang, G., Tang, A., Wang, Y. and An, Z. (2006). Chemical Characteristics of $PM_{2.5}$ and PM_{10} in Haze-Fog Episodes in Beijing. *Environ. Sci. Technol.* 40: 3148–3155.

Turpin, B. J. and Lim, H. J. (2001). Species Contributions to $PM_{2.5}$ Mass Concentrations: Revisiting Common Assumptions for Estimating Organic Mass. *Aerosol Sci. Technol.* 35: 602–610.

Wang, G., Huang, L., Gao, S., Gao, S. and Wang, L. (2002). Characterization of Water-Soluble Species of PM_{10} and $PM_{2.5}$ Aerosols in Urban Area in Nanjing, China. *Atmos. Environ.* 36: 1299–1307.

Wang, Y., Zhuang, G., Tang, A., Yuan, H., Sun, Y., Chen, S. and Zheng, A. (2005). The Ion Chemistry and the Source of $PM_{2.5}$ Aerosol in Beijing. *Atmos. Environ.* 39: 3771–3784.

Wexler, A.S. and Clegg, S.L. (2002). Atmospheric Aerosol Models for Systems including the Ions H^+, NH_4^+, Na^+, SO_4^{2-}, NO_3^-, Cl^-, Br^-, and H_2O. *J. Geophys. Res. Atmos.* 107: ACH 14-1–ACH 14-14.

Xiao, Z.M., Zhang, Y.F., Hong, S.M., Bi, X.H., Jiao, L., Feng, Y.C. and Wang, Y.Q. (2011). Estimation of the Main Factors Influencing Haze, Based on a Long-Term Monitoring Campaign in Hangzhou, China. *Aerosol Air Qual. Res.* 11: 873–882.

Yang, H., Yu, J.Z., Ho, S.S.H., Xu, J., Wu, W.S., Wan, C.H., Wang, X., Wang, X. and Wang, L. (2005). The Chemical Composition of Inorganic and Carbonaceous Materials in $PM_{2.5}$ in Nanjing, China. *Atmos. Environ.* 39: 3735–3749.

Yu, J.Z., Huang, X.F., Xu, J. and Hu, M. (2005). When Aerosol Sulfate Goes Up, so Does Oxalate: Implication For the Formation Mechanisms of Oxalate. *Environ. Sci. Technol.* 39: 128–133.

Zhang, J.P., Zhu, T., Zhang, Q.H., Li, C.C., Shu, H.L., Ying, Y., Dai, Z.P., Wang, X., Liu, X.Y., Liang, A.M., Shen, H.X. and Yi, B.Q. (2012). The Impact of Circulation Patterns on Regional Transport Pathways and Air Quality over Beijing and Its Surroundings. *Atmos. Chem. Phys.* 12: 5031–5053.

Zhang, Q.H., Zhang, J.P. and Xue, H.W. (2010). The Challenge of Improving Visibility in Beijing. *Atmos. Chem. Phys.* 10: 7821–7827.

Zhou, J., Zhang, R., Cao, J., Chow, J.C. and Watson, J.G. (2012). Carbonaceous and Ionic components of Atmospheric Fine Particles in Beijing and their Impact on Atmospheric Visibility. *Aerosol Air Qual. Res.* 12: 492–502.

Received for review, December 19, 2012
Accepted, May 16, 2013